



Optimal Stroke Patterns for Purcell's Three-Link Swimmer

Daniel Tam* and A. E. Hosoi†

Hatsopoulos Microfluids Laboratory, Department of Mechanical Engineering, Massachusetts Institute of Technology, Cambridge, Massachusetts 02139, USA

(Received 10 July 2006; published 9 February 2007)

Stroke patterns for Purcell's three-link swimmer are optimized. We model the swimmer as a jointed chain of three slender rods moving in an inertialess flow. The swimmer is optimized for efficiency and speed. We were able to attain swimmer designs significantly more efficient than those previously suggested by authors who only consider geometric design rather than kinematic criteria. The influence of slenderness on optimality is considered as well.

DOI: [10.1103/PhysRevLett.98.068105](https://doi.org/10.1103/PhysRevLett.98.068105)

PACS numbers: 47.63.mf, 45.40.Ln, 83.60.Yz, 87.19.St

Motivation.—A vast majority of living organisms are unicellular and are found in an astonishing diversity at micrometric scales. This variety is particularly striking when considering motility. The environmental interactions experienced by such microorganisms are fundamentally different from those experienced by larger animals as inertia is irrelevant and the swimming dynamics is dominated by viscosity. The past decade has seen major engineering innovations reaching down to nanometric dimensions, and a growing interest has arisen in exploring new and efficient ways to generate propulsion at these small scales [1,2]. Previous studies have investigated swimming at low Reynolds number analytically [3–5], with a more recent emphasis on efficiency, optimality [1,6–8], and the design of simple swimmers [9,10].

In his famous lecture, *Life at Low Reynolds Number* [11], E. M. Purcell presented what may be the simplest active tail that can effectively propel itself at low Reynolds numbers—the three-link swimmer. This swimmer can be viewed as a simplified and discontinuous flagellum made of three slender rods articulated at two hinges. In a recent study, Becker *et al.* [1] optimized a discrete and limited set of geometric parameters characterizing the infinitely slender three-link swimmer. However, as the authors limited their study to geometric design, the quantitative results given in this work are suboptimal.

Two key ideas separate the current study from previous work by Becker *et al.* as summarized in Table I. The first is the concept of *kinematic* optimization versus *geometric* optimization. Geometric optimization addresses questions related to the geometric design of biological and mechanical swimming devices. In contrast, kinematic optimization confronts the question: Given a swimmer with a particular geometry, what is the optimal actuation strategy? As an analogy, consider an Olympic swimmer. The geometry of the swimmer is fixed but she is physically able to employ any number of strokes: freestyle, breaststroke, butterfly, etc. Kinematic optimization seeks the “best” sequence among this infinite array of possible stroke patterns.

The second significant difference between the present study and previous work is that optimizing kinematics

requires a functional rather than a parametric variation. Unlike the geometric parameters considered in earlier studies, the stroke shape and sequence cannot be described by a single scalar, rather it must be represented by a continuous function (see Fig. 2). Here we extend the results from Becker *et al.* to include kinematics, interactions between the links, and the effects of slenderness to provide a complete description of the optimal three-link swimmer.

Model of the swimmer.—Each link in our swimmer is modeled as a rigid slender body of length $2l$ and radius b with characteristic aspect ratio $\kappa = b/2l$ (see Fig. 1). The Reynolds number is assumed to be small, $\text{Re} = \rho U l / \mu \ll 1$, where U is the characteristic speed of the swimmer, ρ is the fluid density and μ the fluid viscosity. Inertial effects are thus neglected relative to viscous effects, and the hydrodynamics of the system is governed by Stokes equations

$$\nabla \cdot \mathbf{u} = 0, \quad -\nabla p + \mu \nabla^2 \mathbf{u} = \mathbf{0}, \quad (1)$$

subject to the boundary conditions

$$\mathbf{u} = \mathbf{U}_s \text{ on } S, \quad \mathbf{u} \rightarrow \mathbf{0} \text{ at } \infty, \quad (2)$$

where \mathbf{u} and p are the velocity and the pressure fields in the fluid, respectively, and \mathbf{U}_s is the local velocity at the surface, S , of the swimmer. The hydrodynamic forces exerted by the fluid on a slender body are well known as derived by Cox [12]. Let s be the arc length measured along the centerline of the slender swimmer, and $\mathbf{R}, \mathbf{U} \approx \mathbf{U}_s(s), \mathbf{\Lambda}$ and $\hat{\mathbf{R}}, \hat{\mathbf{U}} \approx \mathbf{U}_s(\hat{s}), \hat{\mathbf{\Lambda}}$ the position, velocity, and tangential unit vector of the centerline at s and \hat{s} , respectively (see Fig. 1). The force per unit length \mathbf{f} at s can then be written as

$$\frac{\mathbf{f}}{2\pi\mu} = \left[\frac{-\mathbf{U}}{\ln\kappa} + \frac{\lim_{\epsilon \rightarrow 0} (\mathbf{J} - \mathbf{U} \ln(2\epsilon))}{(\ln\kappa)^2} \right] \cdot [\mathbf{\Lambda}\mathbf{\Lambda} - 2\mathbf{I}] + \frac{-\mathbf{U}}{2(\ln\kappa)^2} \cdot [3\mathbf{\Lambda}\mathbf{\Lambda} - 2\mathbf{I}] + \mathcal{O}\left\{ \frac{1}{(\ln\kappa)^3} \right\}, \quad (3)$$

where

TABLE I. Summary of the parameters optimized in previous work by Becker *et al.* [1] and in the present study.

	Geometry			Kinematics
	Parameter (scalar)	Parameter optimization	Stroke amplitude	Function optimization
	Arm length ratio η	Slenderness $1/\kappa$		Stroke pattern
Becker <i>et al.</i> [1]	$\mathcal{O}(1/(\ln\kappa)^2)$	×	×	
Present study	$\mathcal{O}(1/(\ln\kappa)^3)$	×	×	×

$$\mathbf{J} = -\frac{1}{2} \left[\int_0^{s-2l\epsilon} + \int_{s+2l\epsilon}^{2l} \right] \left[\frac{\mathbf{I}}{|\Delta|} + \frac{\Delta\Delta}{|\Delta|^3} \right] \left[\mathbf{I} - \frac{1}{2} \hat{\Lambda} \hat{\Lambda} \right] \cdot \hat{\mathbf{U}} d\hat{s}, \quad (4)$$

\mathbf{I} is the identity operator and $\Delta \equiv \mathbf{R} - \hat{\mathbf{R}}$.

The swimmer is modeled as an inextensible jointed chain of three cylindrical slender rods of length $2l_i$ (where $i = 1, 2, 3$), whose motion is constrained to be planar. Each link is associated with a position vector \mathbf{X}_i corresponding to 3 degrees of freedom: two translational displacements of the center of the rod and one rotation angle, $\mathbf{X}_i = (x_i, y_i, \theta_i)$ (see Fig. 1). Thus the entire system is completely described by a vector of nine variables: $\mathbf{X} = (\mathbf{X}_1, \mathbf{X}_2, \mathbf{X}_3)$. The velocity vector of each link is defined as $\mathbf{V}_i = \dot{\mathbf{X}}_i$ and the dynamics are subject to the constraint that at each hinge, the velocities of the two neighboring links are equal

$$\begin{bmatrix} \dot{x}_i \\ \dot{y}_i \end{bmatrix} + l_i \dot{\theta}_i (\hat{\mathbf{z}} \times \boldsymbol{\Lambda}_i) = \begin{bmatrix} \dot{x}_{i+1} \\ \dot{y}_{i+1} \end{bmatrix} - l_{i+1} \dot{\theta}_{i+1} (\hat{\mathbf{z}} \times \boldsymbol{\Lambda}_{i+1}), \quad (5)$$

where $\hat{\mathbf{z}}$ is the unit vector out of the plane of motion.

The swimmer's stroke pattern is controlled by imposing the angles between two adjacent links at the hinges, $\Omega_1 = \theta_2 - \theta_1$ and $\Omega_2 = \theta_3 - \theta_2$, which is equivalent to imposing a constraint on the rotational velocities

$$\dot{\Omega}_i = \dot{\theta}_{i+1} - \dot{\theta}_i. \quad (6)$$

The slender body approximation used in this work does not extend to overlapping arm segments; hence, we do not consider self-intersecting stroke patterns.

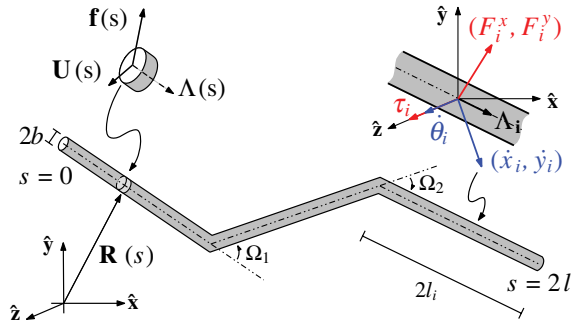


FIG. 1 (color online). Schematic of the swimmer. The slice and corresponding notation on the left refer to the local velocity, tangent vector, and drag force per unit length. Notation on the right refers to the velocity, tangent vector, and force associated with an entire link. Note that (F_i^x, F_i^y) and (\dot{x}_i, \dot{y}_i) lie in the $x - y$ plane while θ_i and τ_i point out of the page in the $\hat{\mathbf{z}}$ direction.

All instantaneous configurations of the swimmer can be represented by a point in the two-dimensional (Ω_1, Ω_2) -phase space. Thus, all periodic stroke patterns of the swimmer can be represented by a single closed curve in this space. A stroke pattern in which only one arm moves at a time appears as a square and will be referred to as the ‘‘Purcell stroke’’ as it is the original pattern proposed by Purcell (see Fig. 2); it is also the only sequence considered in the study by Becker *et al.* [1].

The hydrodynamic forces and torques, $\mathbf{F}_i = (F_i^x, F_i^y, \tau_i)$, on each link are calculated from Eqs. (3) and (4) integrated over each link

$$\mathbf{F}_i = \int_{2l_i} (\mathbf{f} \cdot \hat{\mathbf{x}}, \mathbf{f} \cdot \hat{\mathbf{y}}, \mathbf{R} \times \mathbf{f}) ds = \sum_{j=1}^3 \mathbf{A}_i^j \mathbf{V}_j. \quad (7)$$

As expected from the linearity of Stokes equations, the force vectors take an Aristotelian form and are linear functions of the velocity. The coefficients of the matrix \mathbf{A}_i^j are integrated analytically for $i = j$ and numerically using Gauss quadrature for $i \neq j$.

In the low Reynolds number regime, the swimmer is force- and torque-free. In our case, the slender body only interacts with the surrounding flow and therefore, the integrals of all hydrodynamical forces and torques vanish; thus,

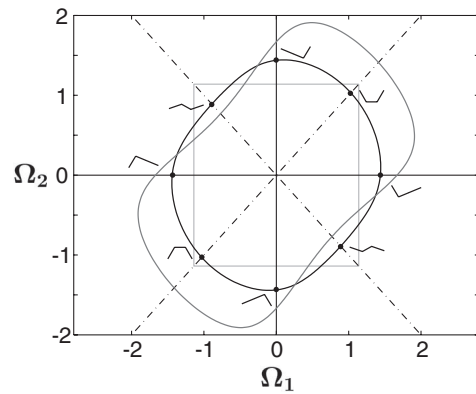


FIG. 2. Stroke sequences of three-link swimmers in the (Ω_1, Ω_2) -phase plane for: (black line) optimal efficiency, (medium gray line) optimal velocity, and (light gray line) the optimal ‘‘Purcell stroke’’ which corresponds to the square. Small swimmer diagrams correspond to successive configurations of the swimmer during the stroke. The swimmer moves to the left when the trajectory is followed counterclockwise and to the right otherwise.

$$\sum_{i=1}^3 \mathbf{F}_i = \sum_{j=1}^3 \left(\sum_{i=1}^3 \mathbf{A}_i^j \right) \dot{\mathbf{X}}_j = \mathbf{0}. \quad (8)$$

Equations (5), (6), and (8) form a system of nine first order differential equations which is integrated using a fourth order Runge-Kutta scheme. It is solved in nondimensional form using the characteristic half-length of an arm link, l_1 , as a reference length, l_{ref} , and the period of the stroke, τ , as a reference time.

Optimality criteria.—In order to find optimal stroke patterns, we first need to determine an objective function, which associates a scalar quantity to each element in the space of feasible strokes. One such function is the distance traveled by the swimmer during one cycle; optimizing this function is equivalent to maximizing the average velocity, V , in the primary direction of motion over one stroke for a given l_{ref} and τ . As each closed curve in the (Ω_1, Ω_2) -phase space can be associated with a unique swimming pattern, this function is well defined.

A second way to characterize the optimality of a swimming stroke is to define an efficiency that measures the fraction of the total energy spent that is used to propel the swimmer in a useful direction. However, this energy-based optimality criterion is dynamic in nature, whereas our system is essentially geometric. The constraints that define the closed curve in phase space do not uniquely restrict the dynamics of the swimmer—as the parametrization along the curve is not specified—and therefore do not uniquely define efficiency. However, it can be shown that there exists a unique parametrization that optimizes efficiency for a given curve. Consider the mechanical power at any given time:

$$\Phi = \int_0^{2l} \mathbf{f} \cdot \mathbf{U} ds = \sum_{i=1}^3 \mathbf{F}_i \cdot \mathbf{V}_i = \mathbf{V}^T \mathbf{A} \mathbf{V}, \quad (9)$$

where \mathbf{A} is obtained by assembling the blocks \mathbf{A}_i^j , and can be shown to be symmetric positive definite. For a given stroke sequence one can demonstrate that the total work, $W = \int \Phi dt$, is minimized for a given parametrization if Φ remains constant over one cycle (see Becker *et al.* [1] for a rigorous proof). It can be further shown that this minimum is attained and unique. Thus, a well-defined minimal work can be associated with every stroke sequence in the (Ω_1, Ω_2) -phase space.

The efficiency criterion, \mathcal{E} , used in this study is similar to that defined in previous work by Lighthill and Purcell and identical to the one used in Becker *et al.* [1]. For a given stroke, the efficiency represents the ratio of the power required to drag the swimmer in its straightened configuration ($\Omega_1 = 0, \Omega_2 = 0$) at its average speed to the average power exerted mechanically against viscosity

$$\mathcal{E} = \frac{4\pi\mu l}{\ln(\frac{2}{\kappa}) - \frac{3}{2}} \frac{V^2}{\Phi}, \quad (10)$$

where V is the swimming speed averaged over one stroke

and Φ is the average optimal mechanical power associated with the stroke.

Optimization procedure.—Without loss of generality, the stroke can be parametrized by two periodic functions Ω_1 and Ω_2 of period τ which can each be represented as a Fourier series. For regular and differentiable functions, the Fourier coefficients decay rapidly and thus our optimization procedure is based on finding the optimal first k coefficients of the series. In addition to the stroke pattern, the geometry of the swimmer is optimized as well. This requires two additional design parameters: the slenderness, $1/\kappa$, and the relative size of the middle link, $\eta = l_2/l_1$. The swimmer is assumed symmetric i.e. $l_1 = l_3$. The optimal solution is found via a gradient search on a finite set of coefficients using the Broyden's quasi-Newton method [13]. Gradients are computed numerically.

Discussion.—Several general observations can be made regarding optimal stroke sequences. First, because of the linearity and time independence of the Stokes equations, we expect optimal strokes to be symmetric with respect to reflections across the axes $\Omega_1 = \Omega_2$ and $\Omega_1 = -\Omega_2$. This can be seen by considering a geometrical configuration where $\Omega_1 = \Omega_2$ in which the two arms are in a symmetric position (see diagrams on Fig. 2). In this configuration, sweeping the right arm down and moving forward in time is indistinguishable from sweeping the left arm down and moving backwards in time. The optimal stroke should be invariant if played backwards in time (time independency) and reflected about the body's line of symmetry (linearity). Hence $\Omega_1 = \Omega_2$ is an axis of symmetry. The second axis of symmetry can be deduced in a similar way, as the arms of the swimmer are also interchangeable in the configuration $\Omega_1 = -\Omega_2$ [14].

These symmetries allow us to consider only one quarter of the optimal curve in a frame $(\hat{\Omega}_1, \hat{\Omega}_2)$ that has been rotated from the original frame by $\pi/4$:

$$\begin{aligned} \hat{\Omega}_1 &= \sum_{p=1, \text{odd}}^{\infty} a_p \cos\left(\frac{2\pi p t}{\tau}\right), \\ \hat{\Omega}_2 &= \sum_{p=1, \text{odd}}^{\infty} b_p \sin\left(\frac{2\pi p t}{\tau}\right). \end{aligned} \quad (11)$$

These axes of symmetry imply that there is no net rotation over one complete stroke cycle, preventing the optimal swimmer from going in circles. In addition, two observations can be made regarding the amplitude of optimal strokes sequences. For small amplitude strokes, both the average speed, V , and the mechanical work, Φ , go to zero. An expansion of the efficiency, \mathcal{E} , shows that it too decays to zero for small Ω_1 and Ω_2 . Thus, regardless of which of the two optimality criteria we choose, small strokes are never desirable. For larger amplitudes, V is bounded while it can be shown that Φ increases quadratically with amplitude; so again, large amplitude strokes are suboptimal. Thus optimal stroke patterns are expected to exist and to

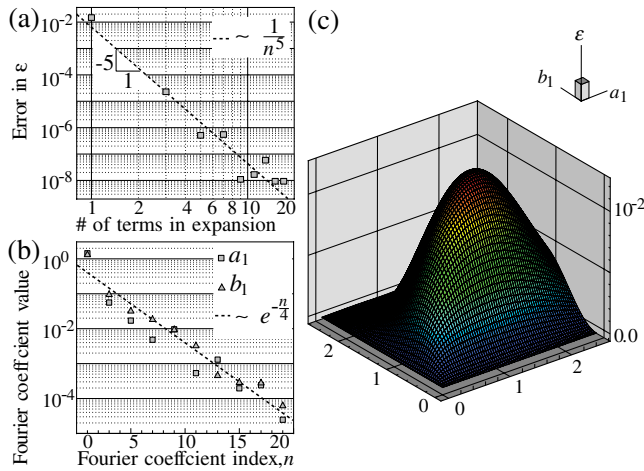


FIG. 3 (color online). (a): Log-log plot of the normalized error in the efficiency as a function of the number of terms in the Fourier series used to find the optimal stroke. (b): Semilog plot showing exponential decay of the amplitude of the Fourier coefficients. (c): Efficiency as a function of the two dominant terms of the Fourier expansion.

be found within a finite ring in the (Ω_1, Ω_2) -phase space centered at the origin.

We first consider the case of an infinitely slender swimmer, $\kappa \rightarrow 0$. Optimal stroke sequences are shown in Fig. 2. The optimal distance stroke corresponds to a dimensionless distance traveled of 0.623 with an efficiency of 0.0093. In comparison, the maximum distance attained with the Purcell stroke is 0.483 with a corresponding efficiency of 0.0063. The difference is even more striking when considering the efficiency criterion. The maximum efficiency reached by the optimized three-link swimmer is 0.0130 (see Fig. 2) for a link ratio of $\eta = 0.747$ and a corresponding dimensionless distance traveled of 0.492; in contrast, the best efficiency achieved with the Purcell stroke is 0.0077 with $\eta = 0.809$ (and a distance of 0.420) as computed in [1]. This represents an increase of 69%, emphasizing the relevance of optimizing kinematics in viscously dominated locomotion [15].

The normalized error in the efficiency decreases rapidly ($\sim 1/n^5$) as the number of Fourier terms is increased [see Fig. 3(a)]. In fact the efficiency of the stroke, computed with only the first term in the expansion, is within 1% of that of the optimal solution. In addition, the coefficients of the Fourier series decay to zero exponentially [see Fig. 3(b)], a signature of a smooth parametrization. These two facts show that the first two terms— a_1 and b_1 in Eq. (11)—largely determine the characteristics of the stroke. Hence we can approximate the properties of the optimal solution by looking at only two coefficients. Figure 3(c) shows that \mathcal{E} is a quasiconvex function with a unique global maximum in this reduced space. Although the optimization procedure only guarantees convergence to a local maximum, this strongly suggests that the global optimum has been achieved.

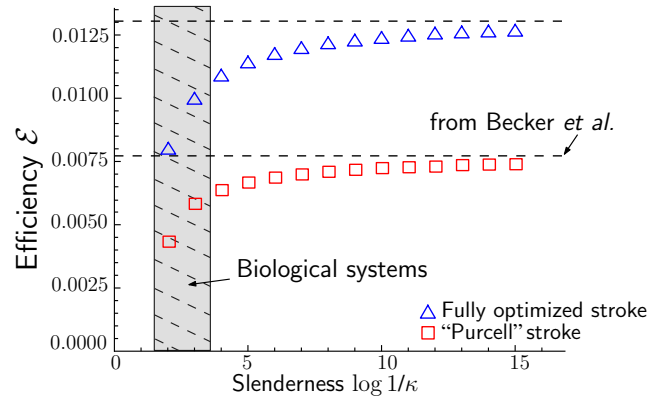


FIG. 4 (color online). Efficiency of the three-link swimmer as a function of slenderness.

Figure 4 shows that efficiency also increases with slenderness, asymptotically approaching the infinite slenderness limit for small values of κ . It is curious to note that there is an abrupt increase in efficiency for dimensionless slenderness less than 10^3 which, although biological systems are clearly more complex than this very simple device, is comparable to the slenderness of the flagella of microorganisms [16].

This work was partially supported by NSF Grant No. CCF-0323672.

*Electronic address: dan_tam@mit.edu

†Electronic address: peko@mit.edu

- [1] L. Becker, S. Koehler, and H. Stone, *J. Fluid Mech.* **490**, 15 (2003).
- [2] R. Dreyfus, J. Baudry, M. Roper, M. Fermigier, H. Stone, and J. Bibette, *Nature (London)* **437**, 862 (2005).
- [3] G. Taylor, *Proc. R. Soc. A* **209**, 447 (1951).
- [4] J. Lighthill, *SIAM Rev.* **18**, 161 (1976).
- [5] G. Hancock, *Proc. R. Soc. A* **217**, 96 (1953).
- [6] A. Shapere and F. Wilczek, *Phys. Rev. Lett.* **58**, 2051 (1987).
- [7] J. Avron, O. Gat, and O. Kenneth, *Phys. Rev. Lett.* **93**, 186001 (2004).
- [8] B. Felderhof, *Phys. Fluids* **18**, 063101 (2006).
- [9] A. Najafi and R. Golestanian, *Phys. Rev. E* **69**, 062901 (2004).
- [10] J. Avron, O. Kenneth, and D. Oaknin, *New J. Phys.* **7**, 234 (2005).
- [11] E. Purcell, *Am. J. Phys.* **45**, 3 (1977).
- [12] R. Cox, *J. Fluid Mech.* **44**, 791 (1970).
- [13] D. Bertsekas, *Nonlinear Programming* (Athena Scientific, Belmont, MA, 2005), 3rd ed.
- [14] Note that this is not the case along the axis $\Omega_1 = 0$ (or $\Omega_2 = 0$) in which the arms can be uniquely identified by their positions relative to the body and hence the symmetry argument fails.
- [15] In comparison, the maximum efficiency of a sinusoidal undulating rod is 0.0736, as calculated by Hancock [5].
- [16] C. Brennen and H. Winet, *Annu. Rev. Fluid Mech.* **9**, 339 (1977).